Bioconjugate Chemistry

Article

pubs.acs.org/bc

Linear–Dendritic Copolymer Composed of Polyethylene Glycol and All-trans-Retinoic Acid as Drug Delivery Platform for Paclitaxel against Breast Cancer

Jianfeng Li,[†] Xutao Jiang,[†] Yubo Guo,[†] Sai An,[†] Yuyang Kuang,[†] Haojun Ma,[†] Xi He,[†] and Chen Jiang*[,†,‡]

[†]Key Laboratory of Smart Drug Delivery (Fudan University), Ministry of Education, Department of Pharmaceutics, School of Pharmacy, Fudan University, 826 Zhangheng Road, Shanghai 201203, China

[‡]State Key Laboratory of Medical Neurobiology, Fudan University, Shanghai 201203, China

Supporting Information

ABSTRACT: A new linear–dendritic copolymer composed of poly(ethylene glycol) (PEG) and all-trans-retinoic acid (ATRA) was synthesized as the anticancer drug delivery platform (PEG-G3-RA_8). It can self-assemble into core–shell micelles with a low critical micelle concentration (CMC) at 3.48 mg/L. Paclitaxel (PTX) was encapsulated into PEG-G3-RA_8 to form PEG-G3-RA_8/PTX micelles for breast cancer treatment. The optimized formulation had high drug loading efficacy (20% w/w of drug copolymer ratio), nanosized diameter (27.6 nm), and narrow distribution (PDI = 0.103). Compared with Taxol, PEG-G3-RA_8/PTX remained highly stable in the serum-containing cell medium and exhibited 4-fold higher cellular uptake. Besides, near-infrared fluorescence (NIR) optical imaging results indicated that fluorescent probe loaded micelle had a preferential accumulation in breast tumors. Pharmacokinetics and biodistribution studies (10 mg/kg) showed the area under the plasma concentration–time curve ($AUC_{0-\infty}$) and mean residence time ($MRT_{0-\infty}$) for PEG-G3-RA_8/PTX and Taxol were 12.006 ± 0.605 mg/L h, 2.264 ± 0.041 h and 15.966 ± 1.614 mg/L h, 1.726 ± 0.097 h, respectively. The tumor accumulation of PEG-G3-RA_8/PTX group was 1.89-fold higher than that of Taxol group 24 h postinjection. With the advantages like efficient cellular uptake and preferential tumor accumulation, PEG-G3-RA_8/PTX showed superior therapeutic efficacy on MCF-7 tumor bearing mice compared to Taxol.

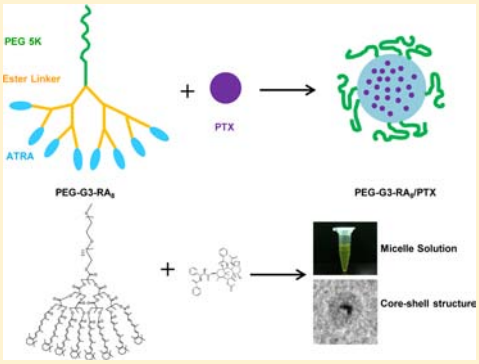

INTRODUCTION

As the development of nanotechnology, many nanoparticles have been investigated for anticancer drug delivery. Among them, polymeric micelles have shown great promise as nanocarriers for efficient drug delivery.[1−3] On one hand, they improve the aqueous solubility of poorly water-soluble chemotherapeutic agents by packing them in the hydrophobic core of the micelles. On the other hand, compared with other delivery systems, micelles show advantages in passive tumor targeting through the leaky vasculature via the enhanced permeability and retention (EPR) effect due to their small size (10–100 nm).[4] However, few of them have been approved by the Food and Drug Administration (FDA).[5] This may be due to their poor stability after administration in vivo. When the concentration of polymers is below the critical micelle concentration (CMC), premature micelles should disassemble and release their payloads quickly.[6] To overcome this drawback, two strategies are often used. One is the covalent linkage between the drug and copolymer or within the copolymer itself. Another one is the rational design of copolymers.[7,8] Among the various copolymers, linear–dendritic copolymers have drawn considerable attention as a promising platform, owing to ease of preparation, low CMC value, good biocompatibility, and relatively high drug loading efficacy.[9−13] The linear–dendritic copolymers usually have one hydrophilic segment and two or more hydrophobic segments. The most used hydrophilic segment was poly(ethylene glycol) (PEG) which could prolong the blood half-lives of micelles. Besides, clinical studies on some drug delivery formulations consisting of PEG have reached phase 2 and 3 stages which indicated the safety of the PEG segment.[14,15] The hydrophobic segment could be designed according to the demand.[11,16]

All-trans-retinoic acid (ATRA) is a natural derivative of vitamin A that has been shown to exert anticancer activities in a number of cancer cells and tissues. It induced growth inhibition, differentiation, and apoptosis of cancer cells.[17−19] Besides, it was demonstrated to sensitize the breast cancer to the cell killing effects of Paclitaxel (PTX) by increasing the phosphorylation of Bcl-2.[20] Here, ATRA was selected as the hydrophobic segment for two reasons. One is the potential synergistic effect mentioned above. The other is the possible low CMC value because of the $\pi-\pi$ interactions between the unsaturated chains of ATRA.[21,22] ATRA was linked to PEG_{5k} via ester bond to form the linear–

Received: October 14, 2014
Published: February 12, 2015

DOI: 10.1021/acs.bioconjchem.5b00030
Bioconjugate Chem. 2015, 26, 418–426

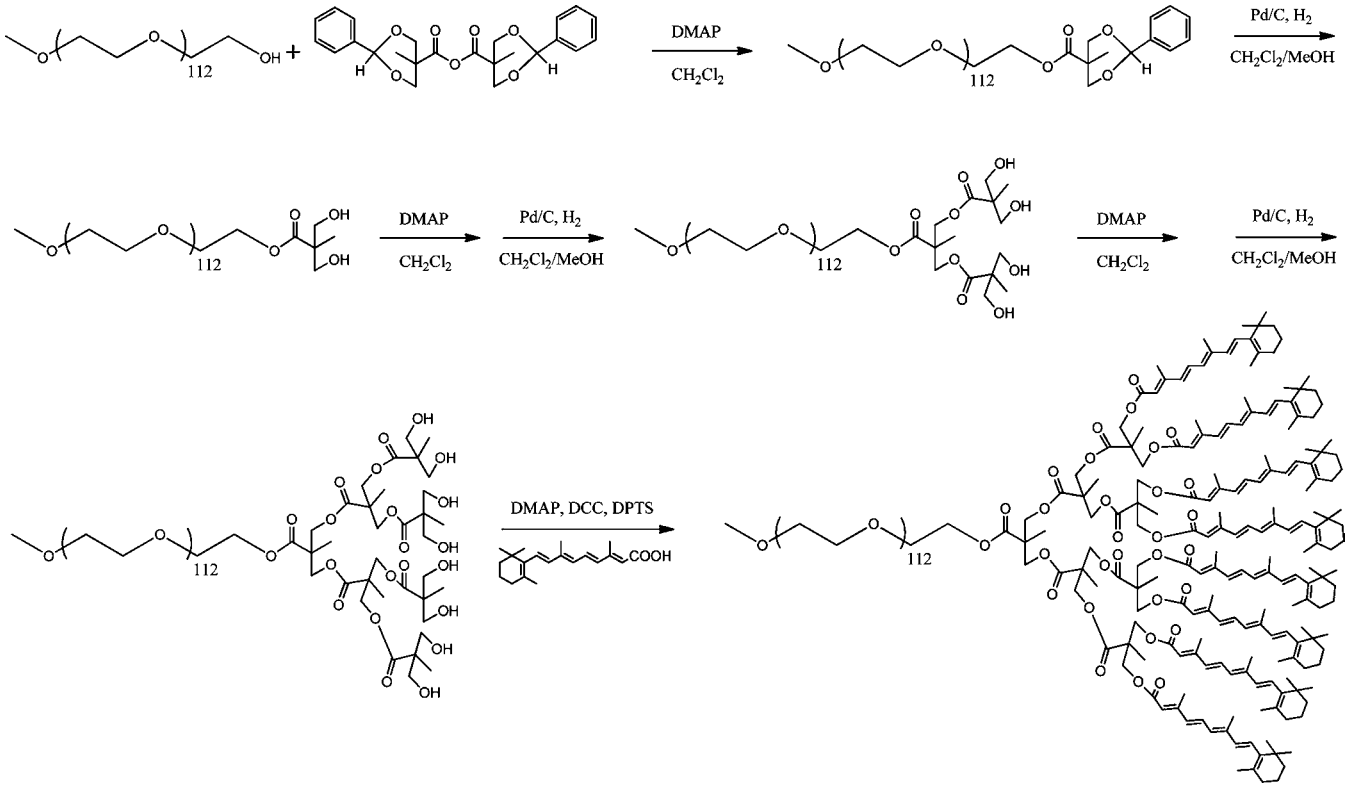

Figure 1. Synthetic route of PEG-G3-RA_8.

dendritic copolymer, PEG-G3-RA_8. PEG-G3-RA_8 was designed as the anticancer drug delivery platform.

PTX is one of first-line chemotherapeutic drugs for the treatment of breast cancer.[23,24] However, its clinical application has been limited due to its poor aqueous solubility. A mixture of Cremophor EL/absolute ethanol (1:1; v/v) was used in the formulation of Taxol to increase its solubility. The relatively large amount of Cremophor EL has been associated with serious side effects, including severe hypersensitivity reactions, myelosuppression, neurotoxicity, and RBC lysis.[25,26] In this study, PTX was encapsulated into PEG-G3-RA_8 for breast cancer treatment to maximize the therapeutic efficacy while minimizing the side effects.

RESULTS AND DISCUSSION

Synthesis and Characterization of PEG-G3-RA_8 Copolymer. At the beginning of this century, Fréchet and his coworkers developed a divergent synthesis of aliphatic ester dendrimers by anhydride coupling. The synthetic route is noteworthy for its rapidity and ability to rapidly produce high-generation aliphatic ester dendrimers of high purity,[27] and the ester bond could be degraded more easily in vivo. Thus, this novel route was applied in our study (Figure 1). In the ^{1}H NMR spectra of PEG-G3-OH_8, peaks around 3.6 ppm represented the repeat units of PEG. Peaks between 1.2 and 1.4 ppm represented H protons of CH_3. The molecular weight of PEG-G3-OH_8 measured via MALDI-TOF was 5742 Da (Supporting Information Figure S1). The ^{1}H NMR spectra of PEG-G3-RA_8 showed the vinyl protons between 5.5 and 6.5 ppm. The molecular weight of PEG-G3-RA_8 was 7185 Da (Supporting Information Figure S2). This indicated 5.12 ATRAs were conjugated to the PEG-G3-OH_8.

As the CMC value was a very important parameter which was related to the stability of the micelle, we hypothesized that the unsaturated chains of ATRA may contribute to the low CMC value because of the $\pi-\pi$ interactions. The CMC value obtained from fluorescent determination was 3.48 mg/L (Figure 2), which

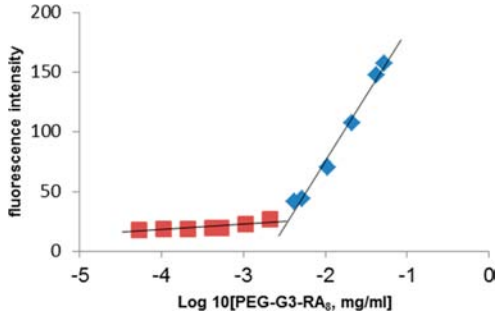

Figure 2. Plot of fluorescence intensity as a function of the logarithm of PEG-G3-RA_8 concentrations using pyrene as a fluorescence probe.

was lower than most polymers reported in the literature.[28,29] Li et al. reported another type of linear−dendritic copolymer composed of PEG, cysteines, and cholic acids.[30] They utilized the cross-linking approach to improve the stability of polymeric micelles. The CMC value of cross-linked copolymer was 0.67 μM (7.5 mg/L), which was along the same order of magnitude as that of PEG-G3-RA_8. This indicated that the rational design proposed here could be a useful method to obtain the copolymers with high stability.

Preparation and Characterization of PTX Loaded Micelles. By evaporation method, PTX can be incorporated into micelles formed by physical entrapment utilizing hydrophobic interactions between PTX and unsaturated chains of

DOI: 10.1021/acs.bioconjchem.5b00030
Bioconjugate Chem. 2015, 26, 418−426

ATRA. Loading efficiency (LE) of PTX into PEG-G3-RA_8 nanoparticles was almost 70% when the initial amount of PTX was <40 wt % of PEG-G3-RA_8, whereas it decreased to 60% when the initial amount increased up to 50 wt % (Figure 3A). The particle size ranged from 27 to 33 nm with narrow distributions. However, when the initial amount increased up to 40 and 50 wt %, large aggregates were found (Supporting Information Figure S3). Thus, the feed ratio of PTX/PEG-G3-RA_8 (% w/w) was set to 30% in the following experiments. The high drug loading efficacy (20 wt %) ensured the reasonable polymer dosage used in in vivo study. The transmission electron microscope (TEM) image showed the core−shell structure of micelles clearly (Figure 3B). Using a dialysis method, Taxol showed a rapid release of 30% of the drug by the first 12 h, after which there was a slow release of 80% of the drug by 72 h. However, PEG-G3-RA_8/PTX was found to exhibit slow drug release into PBS, with cumulative release of 18% of the drug by 72 h (Supporting Information Figure S4). PEG-G3-RA_8/PTX was also found to be stable in 10% fetal bovine serum (FBS) solution. There were slight aggregates when incubated in 20% FBS solution, and higher FBS concentration had a greater effect on the micelle stability (Supporting Information Figure S5).

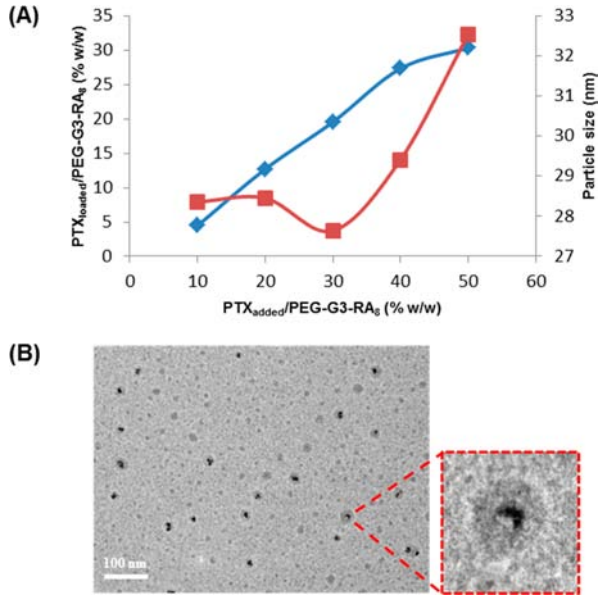

Figure 3. (A) Relationships of the PTX/PEG-G3-RA_8 ratios in micelles (blue line) and the particle size of the micelles (brown line) vs the feed ratios of PTX/PEG-G3-RA_8 during the drug loading, respectively. (B) Transmission electron microscopy (TEM) was performed at the feed ratios of PTX/PEG-G3-RA_8 = 30 (% w/w). The enlarged image showed the core−shell structure of the micelle.

In Vitro Cytotoxicity. The in vitro antitumor activity of PEG-G3-RA_8/PTX against MCF-7 cells was evaluated with an MTT assay. PTX is a very effective mitotic inhibitor used in cancer chemotherapy. The IC_{50} value against different cell lines are usually in the ng/mL range. To ensure the concentration of PEG-G3-RA_8 would be higher than CMC value, the concentration of PTX was set as 1 μg/mL. Besides, a higher PTX concentration (10 μg/mL) was also tested. As shown in Figure 4A, Taxol showed significant cytotoxicity at both concentrations (cell viabilities 24.0 ± 4.2% at 1 μg/mL and 17.2 ± 2.3% at 10 μg/mL). However, PEG-G3-RA_8/PTX was less cytotoxicity than Taxol (cell viabilities 36.8 ± 1.7% at 1 μg/mL and 50.4 ± 9.9% at 10 μg/mL), especially at the concentration of 10 μg/mL. It even worked worse than itself at the concentration of 1 μg/mL. In a previous work, the combination of PTX and ATRA was achieved by incorporating PTX into pullulan acetate and ATRA into PEG-grafted chitosan. The proper PTX/ATRA weight ratio could maximize the synergic effect.[31] However, the synergic effect was not emerged in this system. As shown in the Supporting

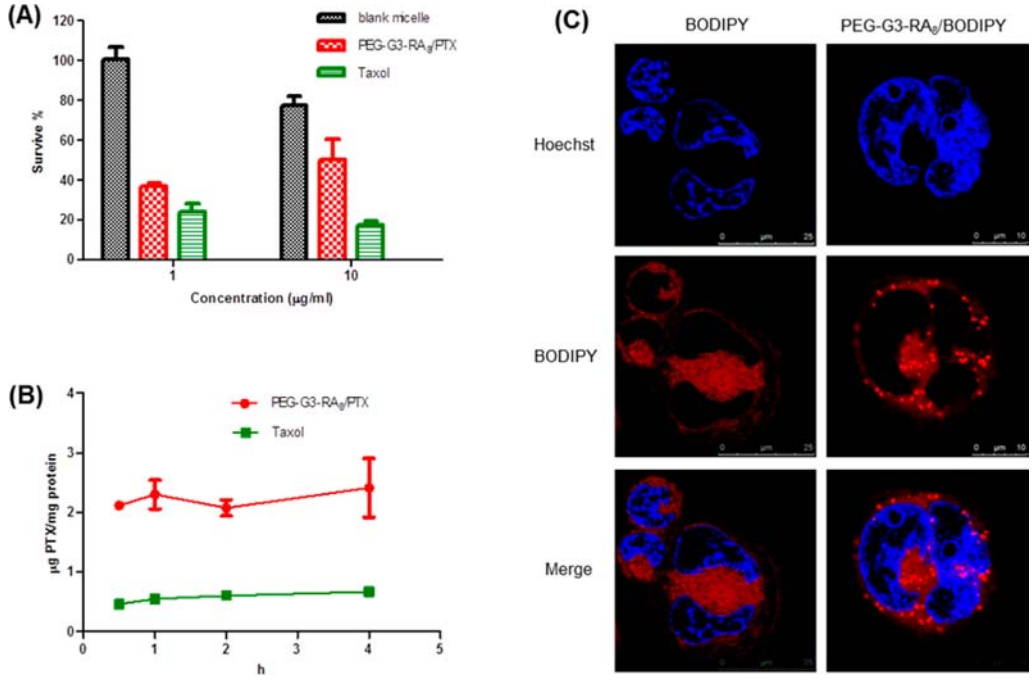

Figure 4. (A) Cytotoxicity of blank micelle, PEG-G3-RA_8/PTX, and Taxol against MCF-7 human breast cancer cells. (B) Time curve of cellular uptake of PEG-G3-RA_8/PTX and Taxol at the PTX concentration of 10 μg/mL. (C) Confocal images of intracellular distribution of BODIPY and PEG-G3-RA_8/BODIPY 24 h after incubation. The nuclei were stained by Hoechst (blue). Data were expressed as mean ± SD (n = 3 or 4).

DOI: 10.1021/acs.bioconjchem.5b00030
Bioconjugate Chem. 2015, 26, 418−426

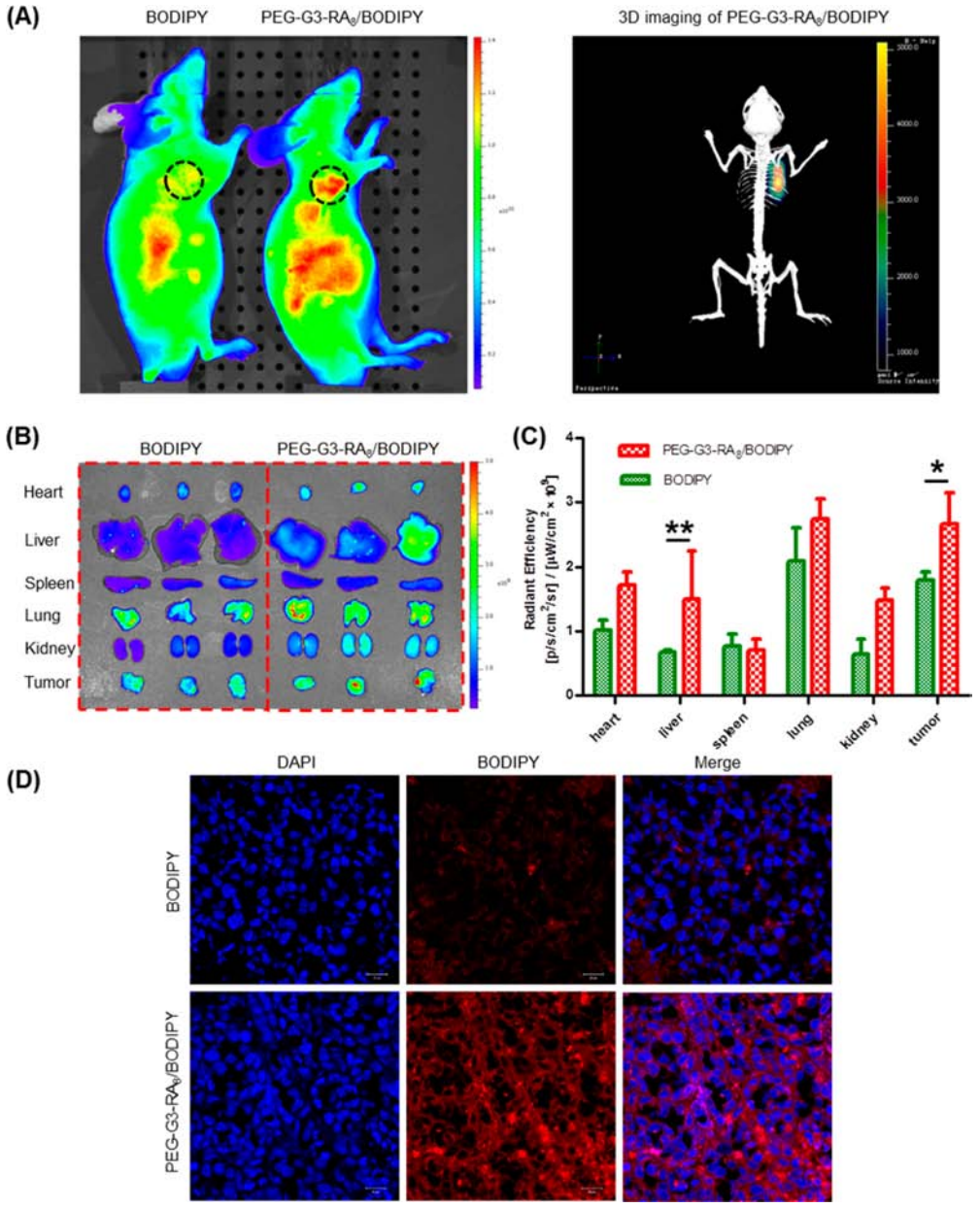

Figure 5. (A) In vivo 2D and 3D imaging 24 h after i.v. injection of BODIPY and PEG-G3-RA_8/BODIPY (0.5 mg/kg) in MCF-7 bearing mice. The optical imaging was obtained using IVIS Spectrum (Ex/Em, 700/729 nm). Black dashed lines indicate the tumor region. (B) Representative ex vivo optical images of tumors and organs of MCF-7 bearing mice sacrificed at 24 h. (C) Quantitative fluorescence intensities of tumors and organs from ex vivo images. Data were expressed as mean ± SD ($n = 3$). *$P < 0.05$ and * *$P < 0.01$. (D) Confocal images of the tumor tissue. The nuclei were stained by DAPI (blue), and red is the signal of BODIPY.

Information Figure S6, PEG-G3-RA_8 was less cytotoxic than ATRA. The slow release profile of the micelles delayed its anticancer activity as compared to free drug ATRA. Besides, it was reported that PTX encapsulated in micelles showed reduced cytotoxicity compared to free PTX regardless of targeting ligand.[29,32]

Cellular Uptake and Intracellular Distribution Studies. The reduced cytotoxicity of micelle formulation may be due to the slow release of PTX from the micelle carrier and/or slow uptake of the micelle formulation by cancer cells. To figure out the cause, the cellular uptake of Taxol and PEG-G3-RA_8/PTX was determined by HPLC. Both formulations showed rapid cellular uptake and reached their plateau after 0.5 h (Figure 4B). This was consistent with Edward H. Kerns' work in which the concentration of paclitaxel rapidly increased in cells upon introduction into the medium, reaching steady state within 5 min.[33] However, the cellular uptake amount of PEG-G3-RA_8/PTX was almost 4-fold higher than that of Taxol (2.41 ± 0.49 versus 0.67 ± 0.04 μg PTX/mg protein) after 4 h incubation. This indicated that the reduced cytotoxicity was in relation to the release profile of PTX.

We then supposed that PTX was released slowly from PEG-G3-RA_8/PTX due to the strong interaction between aromatic rings of PTX and unsaturated chains of ATRA. To validate this point, an intracellular distribution study was carried out using a confocal microscopy. The fluorescent dye BODIPY with long wavelength of excitation and emission (Ex/Em, 700/729 nm) was loaded into the micelle. As shown in Figure 4C, cells exposed

DOI: 10.1021/acs.bioconjchem.5b00030
Bioconjugate Chem. 2015, 26, 418−426

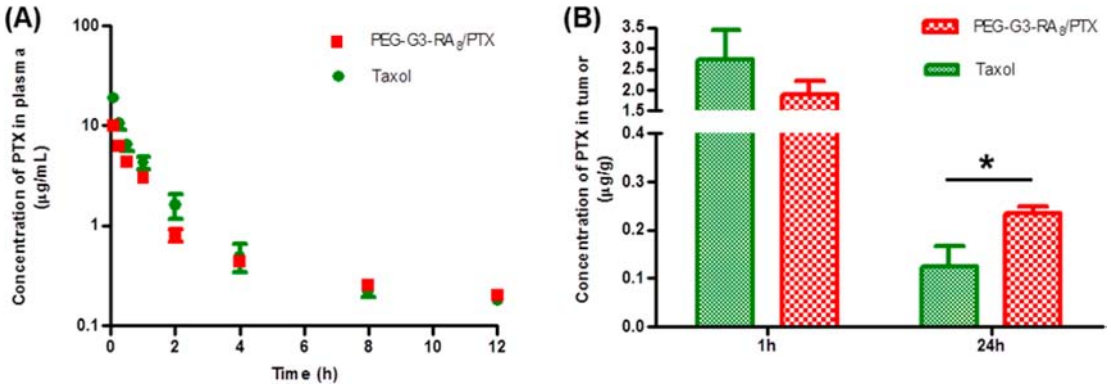

Figure 6. (A) Concentration of PTX in rat plasma after i.v. injection of Taxol and PEG-G3-RA_8/PTX at a dose of 10 mg/kg ($n = 6$). (B) Concentration of PTX in MCF-7 bearing mice 1 and 24 h after receiving the same treatment ($n = 4$). Data were presented as mean ± SD, $^*P < 0.05$.

to free BODIPY showed dispersive distribution in the whole cytoplasm 24 h after incubation. In contrast, cells exposed to BODIPY-loaded micelles had a punctate fluorescence in the cytoplasm, consistent with the results of other studies.[34,35] These observations suggest that the micelles were stable in the presence of cells and serum-containing cell medium. This was consistent with the stability results that micelles were stable in 10% FBS solution (the cell medium also contained 10% FBS). Besides, the in vitro release profile showed that less than 20% of the drug was released. Taken together, the low CMC value was like a double-edged sword. In one aspect, it could increase the stability of the micelle. In another aspect, the slow release profile of incorporated drug could decrease its cytotoxicity against tumor cell and bury the potential synergic effect.

In Vivo Biodistribution of PEG-G3-RA_8/BODIPY Micelle in MCF-7 Bearing Mice. Near infrared fluorescence (NIR) optical imaging technology was utilized to monitor the in vivo 2D and 3D distribution and tumor targeting efficiency of BODIPY loaded PEG-G3-RA_8/BODIPY micelles in MCF-7 bearing mice. An equivalent amount of free BODIPY dye or PEG-G3-RA_8/BODIPY was injected via the tail vein at a dose of 0.5 mg/kg. In Figure 5A, mice administered with PEG-G3-RA_8/BODIPY showed more accumulation of BODIPY 24 h post injection. After that, tumors and major organs were excised for ex vivo imaging to determine the tissue distribution (Figure 5B,C). PEG-G3-RA_8/BODIPY mainly accumulated in the tumor tissue (2.66 ± 0.49 $[p/s/cm^2/sr]/[\mu W/cm^2 \times 10^9]$), which exhibited strong NIR fluorescence intensity, 1.5-fold higher than the tumor uptake of free BODIPY (1.79 ± 0.12 $[p/s/cm^2/sr]/[\mu W/cm^2 \times 10^9]$). Confocal images of the tumor tissue also revealed that the tumor accumulation of PEG-G3-RA_8/BODIPY was more than that of the free BODIPY (Figure 5D). This was likely due to the EPR effects and fast cellular uptake of micelles. Besides, the fluorescence intensity of PEG-G3-RA_8/BODIPY group was significantly higher than that of free BODIPY group (1.51 ± 0.74 vs 0.67 ± 0.04 $[p/s/cm^2/sr]/[\mu W/cm^2 \times 10^9]$) in the liver. This indicated that particles larger than the renal cutoff size (10 nm) were eliminated predominately via reticuloendothelial system uptake such as Kupffer cells in the liver.[1]

Pharmacokinetics and Biodistribution Studies. To quantitatively evaluate the in vivo biodistribution of PEG-G3-RA_8/PTX, the PTX concentration in plasma was measured after i.v. injections of PEG-G3-RA_8/PTX and Taxol. The pharmacokinetic profiles (10 mg/kg, equal to PTX) are illustrated in Figure 6A and the pharmacokinetic parameters were obtained using noncompartmental model fitting. The area under the plasma concentration−time curve ($AUC_{0-\infty}$) and mean residence time ($MRT_{0-\infty}$) for PEG-G3-RA_8/PTX and Taxol were 12.006 ± 0.605 mg/L h, 2.264 ± 0.041 h and 15.966 ± 1.614 mg/L h, 1.726 ± 0.097 h, respectively. Although the plasma concentration of PTX for PEG-G3-RA_8/PTX was lower than that of Taxol after the first 2 h, it went slightly higher than that of Taxol at later time points. It was reported that Taxol is a Cremophor EL (surfactant) formulation of paclitaxel, and can also form micelles of about 10 nm in size upon dilution in water or biological fluids.[36] This may explain the high initial plasma concentrations of Taxol. However, the therapeutic window of PTX was between the side-effect level (8540 ng/mL) and the minimum effective level (43 ng/mL).[24] Thus, high initial plasma concentration of PTX together with relatively large amount of Cremophor induced serious side effects.

The tumor accumulation was investigated in MCF-7 bearing mice 1 and 24 h after i.v. injections of PEG-G3-RA_8/PTX and Taxol at a dose of 10 mg/kg equal to PTX. The relatively high initial plasma concentration of PTX for Taxol led to slightly higher tumor accumulation than that of PEG-G3-RA_8/PTX group at the first 1 h, while the tumor accumulation of PEG-G3-RA_8/PTX group was 1.89-fold higher than that of Taxol group at 24 h. The high stability of PEG-G3-RA_8/PTX contributed to the prolonged retention time. Taken the high cellular uptake together, PEG-G3-RA_8/PTX showed preferable tumor accumulation which was consistent with the results of NIR imaging.

Therapeutic Study. The antitumor effects of PEG-G3-RA_8/PTX were evaluated in MCF-7 bearing mice. Saline, Taxol (10 mg/kg), and PEG-G3-RA_8/PTX (5 and 10 mg/kg, equal to PTX) were administered on days 0, 4, 8, and 12. Compared with the control group, mice in all the treatment groups displayed significantly slower increased rates of tumor growth (Figure 7B,C). Low dose group treated with PEG-G3-RA_8/PTX (5 mg/kg) showed comparable tumor inhibition to the Taxol treated group, and the high dose group treated with PEG-G3-RA_8/PTX (10 mg/kg) demonstrated superior antitumor activity as compared with the Taxol treated group, which may be due to the low CMC value and the preferable tumor accumulation. Terminal deoxynucleotidyl transferase dUTP nick end labeling (TUNEL) assay was also carried out to evaluate the antitumor effect of PTX-loaded micelles. As shown in Supporting Information Figure S7, PEG-G3-RA_8/PTX (10 mg/kg) treated group showed more significant tumor apoptosis than the Taxol treated group, and the PEG-G3-RA_8/PTX (5 mg/kg) treated group showed comparable apoptosis to the Taxol-treated group.

DOI: 10.1021/acs.bioconjchem.5b00030
Bioconjugate Chem. 2015, 26, 418−426

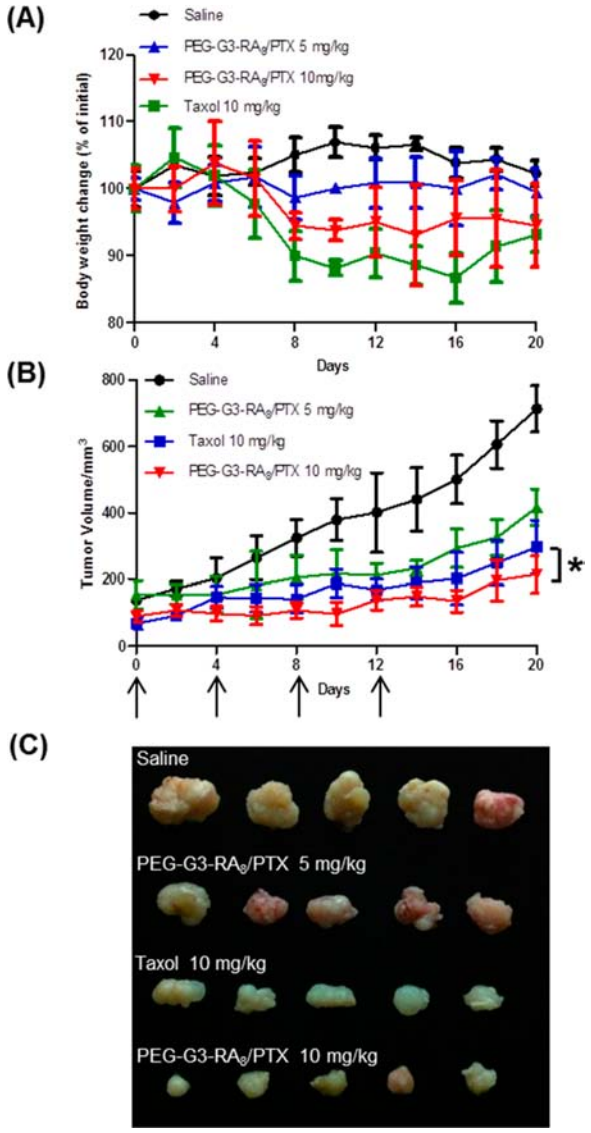

Figure 7. Antitumor efficacy of PEG-G3-RA_8/PTX on MCF-7 bearing nude mice. The tumor volume (A) and body weight change (B) after i.v. injections of Taxol (10 mg/kg) and PEG-G3-RA_8/PTX (5, 10 mg/kg) on days 0, 4, 8, and 12 (saline served as control). At day 20, mice were sacrificed and tumors were imaged (C). Data were presented as mean ± SD (n = 5), *P < 0.05.

Toxicities were assessed by analyzing effects on body weight change monitored every other day (Figure 7A). The Taxol treated group exhibited significant body weight loss during the treatment course, while both PEG-G3-RA_8/PTX treated groups showed no obvious body weight change. In addition, H&E staining of main organs was analyzed to evaluate the toxicity of different PTX formulations. As compared to the saline treated group, there was no histological evidence of side effects in any of the micelle treated groups, while there was some inflammatory infiltration in the liver and kidney of the Taxol treated group which was caused by Cremophor EL (Supporting Information Figure S8). Thus, linear−dendritic copolymer could be a safe PTX delivery platform.

CONCLUSION

In summary, a new linear−dendritic copolymer composed of PEG and ATRA was successfully synthesized with advantages like easy synthetic route, easy purification, and high yield. PEG-G3-RA_8 can readily encapsulate hydrophobic drugs such as PTX with high drug loading efficacy, which can significantly reduce the copolymer dose for in vivo application. The self-assembled micelle was highly stable regardless of the presence of cells and serum-containing cell medium. PEG-G3-RA_8/PTX had efficient cellular uptake and preferential accumulation in breast tumors, which resulted in enhanced therapeutic efficacy with better safety when compared to Taxol. Therefore, the PEG-G3-RA_8 based micelle formulation is a promising hydrophobic drug delivery platform for cancer therapy.

MATERIALS AND METHODS

Materials. MeO-PEG-OH (MW 5 kDa) was purchased from Yuanye Technology (Shanghai, China). PTX was obtained from melonepharma (Dalian, China). Fluorescent dye BODIPY was synthesized according to the literature.[37] Other reagents, if not specified, were purchased from Sigma-Aldrich and used without purification.

Synthesis of PEG-G3-RA_8 Copolymer. PEG-G3-OH_8 was synthesized as reported by Henrik Ihre et al.[27] In brief, MeO-PEG-OH with a molecular weight of 5 kDa (2.0 g, 1 equiv) was dissolved in 6 mL of CH_2Cl_2. Benzylidene-2,2-bis(oxymethyl)-propionic anhydride (0.35 g, 2 equiv) and 4-dimethylaminopyridine (DMAP) (20 mg, 0.4 equiv) was added. Then, the reaction mixture was stirred for 6 h at room temperature. The excess anhydride was quenched by adding 1 mL of MeOH. After stirring for another 5 h, the mixture was precipitated into 300 mL of diethyl ether. The precipitate was filtered to afford 1.97 g of product as a white powder. The benzylidene protection was removed by H_2 reduction. The product was dissolved in 12 mL of a 1:2 mixture of CH_2Cl_2 and MeOH. The catalyst (Pd/C 10%) was added to the reaction mixture followed by stirring under H_2 atmosphere. After removal of the catalyst by filtration, the product was precipitated into 300 mL of diethyl ether, affording 1.73 g of MeO-PEG-G1-OH_2.

MeO-PEG-G1-OH_2 (1.73 g, 1 equiv) was dissolved in 6 mL of CH_2Cl_2. Benzylidene-2,2-bis(oxymethyl)propionic anhydride (1.15 g, 8 equiv) and DMAP (65 mg, 1.6 equiv) was added. Then, the reaction mixture was stirred for 15 h at room temperature. The excess anhydride was quenched by adding 1.08 mL of MeOH. After stirring for another 7 h, the mixture was precipitated into 300 mL of diethyl ether. The precipitate was filtered to afford 1.78 g of product as a white powder. The benzylidene protection was removed as described above and afforded 1.6 g of MeO-PEG-G2-OH_4.

MeO-PEG-G2-OH_4 (1.6 g, 1 equiv) was dissolved in 11 mL of CH_2Cl_2. Benzylidene-2,2-bis(oxymethyl)propionic anhydride (2.5 g, 20 equiv) and DMAP (72 mg, 2 equiv) was added. Then, the reaction mixture was stirred for 18 h at room temperature. The excess anhydride was quenched by adding 1.5 mL of MeOH. After stirring for another 8 h, the mixture was precipitated into 300 mL of diethyl ether. The precipitate was filtered to afford 1.7 g of product as a white powder. The benzylidene protection was removed as described above and afforded 1.45 g of MeO-PEG-G3-OH_8. It was characterized by ^{1}H NMR and gel MALDI-TOF MS. ^{1}H NMR spectra were recorded on a Bruker AMX-400 NMR spectrometer, using tetramethylsilane (TMS) as an internal standard and $CDCl_3$ as solvent.

4-(Dimethy1amino)pyridinium 4-toluenesulfonate (DPTS) was used as catalyst for the efficient polyesterification.[38] MeO-PEG-G3-OH_8 was dissolved in 30 mL of CH_2Cl_2 (1.2 g, 1 equiv).

DOI: 10.1021/acs.bioconjchem.5b00030
Bioconjugate Chem. 2015, 26, 418−426

All-trans-retinoic acid (1.224 g, 20 equiv), DPTS (300 mg, 5 equiv), DMAP (125 mg, 5 equiv), and *N,N′*-dicyclohexylcarbodiimide (DCC) (1.26 g, 30 equiv) were added. The reaction mixture was stirred for 24 h at room temperature. The product was purified by dialysis against *N,N*-dimethylformamide (DMF) using a Spectra/Por 6 membrane with a 5000 MWCO, followed by distillation of the DMF to afford 1.1 g of PEG-G3-RA_8. The final product was characterized by ^{1}H NMR and MALDI-TOF MS as described above.

Critical Micelle Concentration (CMC). Pyrene was used as a fluorescent probe to determine the CMC of PEG-G3-RA_8. When the concentration of PEG-G3-RA_8 was above the CMC, pyrene would be incorporated into the core of the micelle. The fluorescence intensity (Ex = 334 nm, Em = 480 nm) would increase along with the PEG-G3-RA_8 concentration. A 10 μL of pyrene stock solution (2×10^{-4} M in acetone) was added into empty vials and the solvent was evaporated at 37 °C. After evaporation, vials were filled with 1 mL of PEG-G3-RA_8 solution at a fixed concentration and gently stirred overnight at room temperature to ensure pyrene incorporation into micelles. The fluorescence intensity was calculated and plotted as a function of PEG-G3-RA_8 concentration. The CMC was determined from the inflection point of the plot of the fluorescence intensity versus logarithm of PEG-G3-RA_8 concentration. Using linear regression, the equations describing the two linear parts of the plot were established. The CMC was then obtained from the intersection of these two lines.

Preparation and Characterization of PTX Loaded Micelles. The evaporation method was used for PTX loading. In brief, PTX and polymer were dissolved in dichloromethane, evaporated in a rotavapor, and dried under vacuum to obtain a dry film. The film was reconstituted in PBS buffer, followed by sonication for 0.5 h, allowing the polymer to self-assemble into PEG-G3-RA_8/PTX micelles. Finally, the micelle solution was filtered with a 0.22 μm filter to sterilize the sample and stored at 4 °C. The concentration of PEG-G3-RA_8 was measured by UV absorption at 350 nm. High-performance liquid chromatography (HPLC) for PTX quantification was performed on a Waters HPLC system with a reverse phase C18 column (250 × 4.6 mm, 5 μm). The mobile phase consisted of acetonitrile/water 60:40 (v/v) and at a flow rate of 1 mL/min. The injected volume was 20 μL. A UV detector (Waters 2487) was set to monitor at 227 nm. The calibration curve was generated using PTX solutions between 78.125 and 10 000 ng/mL in MeOH, and a good linear correlation (r^2 = 0.9992) was obtained. All quantifications were performed in triplicate.[39] The mean diameter and size distribution of micelles were evaluated by dynamic light scanning (Zetasizer, Nano-ZS, Malvern, UK). The morphology of micelles was observed using transmission electron microscope (Tecnai G2 spirit Biotwin, FEI).

To determine the in vitro drug release profile, Taxol and PEG-G3-RA_8/PTX micelles were diluted with PBS buffer (pH 7.4) to an equal PTX concentration of 1 mg/mL (2 mL) and placed into dialysis bags with MWCO of 3500 Da (Spectra/Por 7, Spectrum Laboratories Inc.). The bags were submerged into a bottle containing 200 mL of release medium (PBS buffer and 0.5% v/v of Tween 80) inside a 37 °C air bath while being shaken at 100 rpm. The solution from the release medium (1 mL) was withdrawn at the selected time points and replaced with 1 mL fresh PBS buffer. The PTX concentration was measured by HPLC.

The stability study was performed to monitor the change in particle size of PEG-G3-RA_8/PTX in the presence of different FBS solutions for the designed time points.

In Vitro Cytotoxicity. MCF-7 cells were obtained from American Type Culture Collection (ATCC, Rockville, MD, USA) and cultured at 37 °C in a humidified 5% CO_2 atmosphere. Growth medium was Dulbecco's modified Eagle's Medium (DMEM) which supplemented with 10% fetal bovine serum (FBS), 100 U/mL penicillin, and 100 μg/mL streptomycin. After the optimization of micelle formulation, the feed ratio of PTX/PEG-G3-RA_8 was set at 30 (% w/w). The cytotoxicity of Taxol, blank micelle, and PEG-G3-RA_8/PTX micelle on MCF-7 cells was evaluated by methlythiazolyltetrazolium (MTT) assay.[40] Taxol and PEG-G3-RA_8/PTX micelle were diluted with DMEM medium containing 10% FBS. The final concentration of PTX in both formulations was assigned to 1 and 10 μg/mL. Cells were exposed to both formulations at 37 °C for 48 h. Then, cells were washed with PBS. To assess cell viability, 200 μL of MTT (0.5 mg/mL) solution was added into each well and incubated at 37 °C for 4 h. The medium was removed and 100 μL of DMSO was added to each well to dissolve the formazan crystals formed by the living cells. Cells without treatment served as control. Cells were also incubated with blank micelle at the equivalent polymer concentration. Absorbance was read at 570 nm and corrected at 630 nm by dual wavelength detection using a Multiscan MK3 microplate reader (Thermo Scientific). Cell viability was calculated as the survival percentage of control.

Quantitative Analysis of Cellular Uptake by HPLC. The cellular uptake of Taxol and PEG-G3-RA_8/PTX was further evaluated in MCF-7 cells via HPLC. Cells were seeded onto 12-well plates at a density of 10^6 cells per well and maintained for 24 h at 37 °C. Cells were then treated with 0.7 mL of Taxol and PEG-G3-RA_8/PTX solution (10 μg/mL equivalent PTX concentration) for different times. After treatment, cells were then washed twice with PBS and 0.5 mL of ddH_2O was added. Sonication was used to rupture the cells. The solution was then centrifugated at 12 000 rpm for 5 min to remove the cell debris. Twenty-five microliters of the supernatant were used for the messurement of protein concentration by BCA Protein Assay Kit. Meanwhile, 0.1 mL of MeOH was added into another 0.1 mL of supernatant to release the PTX from micelles and precipitate most proteins. Then, the solution was centrifugated again at 12 000 rpm for 5 min. The final solution was used for the measurement of PTX concentration by HPLC.

Intracellular Distribution of BODIPY and PEG-G3-RA_8/BODIPY. Julie Murtagh et al. reported a class of BF_2-chelated tetraarylazadipyrromethene fluorophore with excellent absorption and fluorescence properties in the 650−750 nm spectral region.[41] The tetraaryl analogue **1** (BODIPY) has an excitation λ_{max} at 700 nm and emission at 729 nm in water. The long wavelength of excitation and emission light was excellent in both in vitro and in vivo optical imaging. To trace the intracellular distribution of micelles, BODIPY (1% w/w) and PTX were coloaded using the same method described as above. The concentration of BODIPY was measured by UV absorption at 705 nm. The free BODIPY was dissolved in a mixture of Cremophor EL and anhydrous ethanol (1:1, v/v). After incubation for 24 h, MCF-7 cells were examined using a confocal microscopy (LeicalTCS SP2 AOBS, Germany).

In Vivo Biodistribution of PEG-G3-RA_8/BODIPY Micelle in MCF-7 Bearing Mice. Female Balb/c nude mice of about 20 g body weight were purchased from the Department of Experimental Animals, Fudan University and maintained under

DOI: 10.1021/acs.bioconjchem.5b00030
Bioconjugate Chem. 2015, 26, 418−426

standard housing conditions. All animal experiments were carried out in accordance with guidelines evaluated and approved by the ethics committee of Fudan University. When establishing the tumor model, the nude mice was treated with estrogen. The 17-β-estradiol-sustained release pellets (0.72 mg, 60-day release, Innovative Research of America) were implanted subcutaneously into the right back between the ear and the shoulder.[42] After 3 days, 5×10^6 MCF-7 cells suspended in 100 μL PBS was inoculated in the right mammary fat pad. Mice with tumors of an approximate 300 mm^3 were subjected to in vivo imaging. Free BODIPY and PEG-G3-RA_8/BODIPY were injected intravenously via the tail vein in tumor bearing mice at a BODIPY dose of 0.5 mg/kg. After 24 h, mice were anaesthetized by 1% isoflurane/oxygen mixture and then scanned using IVIS Spectrum with Living Image software v 4.2 (Caliper Life Science). After in vivo imaging, mice were anesthetized with diethyl ether and killed by decapitation. Tumors and organs were excised and imaged.

For histological evaluation, excised tumor fixed in 4% paraformaldehyde for 48 h. Then, tumors were frozen in OCT embedding medium (Sakura, Torrance, CA, USA) at −80 °C. Frozen sections of 20 μm thickness were prepared with a cryotome Cryostat (Leica, CM 1900, Wetzlar, Germany) and stained with 300 nM DAPI for 10 min at room temperature. The slides were mounted with coverslips and visualized with confocal microscopy.

Pharmacokinetics and Biodistribution Studies. The pharmacokinetics of Taxol and PEG-G3-RA_8/PTX were determined in SD rats. These two formulations were administered intravenously via the tail vein at a dose of 10 mg/kg ($n = 6$). The blood samples of each group were collected in heparinized tubes at different time point (0.083, 0.25, 0.5 1, 2, 4, 8, 12 h). Liquid−liquid extraction method was used for extraction of PTX from plasma samples. Drug concentration was subsequently quantified by HPLC. Briefly, 50 μL of docetaxel (5 μM in MeOH) was added to 50 μL of plasma sample as an internal standard (IS). One milliliter of anhydrous diethyl ether was then added and the mixture was vortexed for 2 min. Following centrifugation (12 000 rpm, 5 min), supernatant was transferred to another tube and the solvent was dried under a stream of nitrogen at 40 °C. Dried samples were reconstituted with MeOH, vortexed for 60 s, and centrifuged at 12 000 rpm, for 5 min. Twenty microliters of each sample was injected into HPLC column for PTX quantification.

The biodistribution study was performed in nude mice with tumors of approximately 300 mm^3. Taxol and PEG-G3-RA_8/PTX were administered intravenously via the tail vein at a dose of 10 mg/kg ($n = 4$). At time point 1 and 24 h, mice were sacrificed. Tumors were collected, washed with cold saline, dried over filter paper, weighed, and frozen at −20 °C until analysis. The PTX concentration in 10% (w/v) tumor homogenate was measured by LC/MS as described elsewhere.[43]

Therapeutic Study. The therapeutic efficacy was evaluated in MCF-7 bearing nude mice. Treatments were started when tumor reached a volume of 100−200 mm^3, and this day was designated as day 0. Mice were randomly divided into four groups ($n = 5$). Mice were administered intravenously with Taxol (10 mg/kg), PEG-G3-RA_8/PTX (5, 10 mg/kg), and saline on days 0, 4, 8, and 12. Body weight of mice and tumor volume were measured every other day. Tumor volume was calculated by the formula $\pi/6 \times LW^2$, where L is the long diameter and W is the short diameter.

Statistical Analysis. The pharmacokinetic parameters were calculated using noncompartmental analysis with DAS 2.0 software. Data are represented as mean ± S.D. For statistical analyses, GraphPad Prism software (v 5.0) was used. Groups were compared using unpaired t test. A value of $P < 0.05$ was considered statistically significant.

■ ASSOCIATED CONTENT

Supporting Information

Characterization of PEG-G3-OH_8 and PEG-G3-RA_8, optimization of micelle formulation, in vitro PTX release profiles, and stability of micelles. This material is available free of charge via the Internet at http://pubs.acs.org.

■ AUTHOR INFORMATION

Corresponding Author

*E-mail: jiangchen@shmu.edu.cn. Tel: +86-21-5198-0079. Fax: +86-21-5198-0079.

Notes

The authors declare no competing financial interest.

■ ACKNOWLEDGMENTS

This work was supported by the grant from National Basic Research Program of China (973 Program, 2013CB932500), National Natural Science Foundation of China (81172993), and National Science Fund for Distinguished Young Scholars (81425023).

■ REFERENCES

(1) Hou, L., Yao, J., Zhou, J., and Zhang, Q. (2012) Pharmacokinetics of a paclitaxel-loaded low molecular weight heparin-all-trans-retinoid acid conjugate ternary nanoparticulate drug delivery system. *Biomaterials 33*, 5431−5440.

(2) Wang, X., Wu, G., Lu, C., Zhao, W., Wang, Y., Fan, Y., Gao, H., and Ma, J. (2012) A novel delivery system of doxorubicin with high load and pH-responsive release from the nanoparticles of poly (alpha,beta-aspartic acid) derivative. *Eur. J. Pharm. Sci. 47*, 256−264.

(3) Nishiyama, N., and Kataoka, K. (2001) Preparation and characterization of size-controlled polymeric micelle containing cis-dichlorodiammineplatinum(II) in the core. *J. Controlled Release 74*, 83−94.

(4) Gao, G. H., Li, Y., and Lee, D. S. (2013) Environmental pH-sensitive polymeric micelles for cancer diagnosis and targeted therapy. *J. Controlled Release 169*, 180−184.

(5) Davis, M. E., Chen, Z. G., and Shin, D. M. (2008) Nanoparticle therapeutics: an emerging treatment modality for cancer. *Nat. Rev. Drug Discovery 7*, 771−782.

(6) Wei, X., Wang, Y., Zeng, W., Huang, F., Qin, L., Zhang, C., and Liang, W. (2012) Stability influences the biodistribution, toxicity, and anti-tumor activity of doxorubicin encapsulated in PEG-PE micelles in mice. *Pharm. Res. 29*, 1977−1989.

(7) Cheng, L., and Cao, D. (2009) Effect of tail architecture on self-assembly of amphiphiles for polymeric micelles. *Langmuir 25*, 2749−2756.

(8) Suek, N. W., and Lamm, M. H. (2008) Computer simulation of architectural and molecular weight effects on the assembly of amphiphilic linear-dendritic block copolymers in solution. *Langmuir 24*, 3030−3036.

(9) Xiao, K., Luo, J., Fowler, W. L., Li, Y., Lee, J. S., Xing, L., Cheng, R. H., Wang, L., and Lam, K. S. (2009) A self-assembling nanoparticle for paclitaxel delivery in ovarian cancer. *Biomaterials 30*, 6006−6016.

(10) Huang, Y., Lu, J., Gao, X., Li, J., Zhao, W., Sun, M., Stolz, D. B., Venkataramanan, R., Rohan, L. C., and Li, S. (2012) PEG-derivatized embelin as a dual functional carrier for the delivery of paclitaxel. *Bioconjugate Chem. 23*, 1443−1451.

DOI: 10.1021/acs.bioconjchem.5b00030
Bioconjugate Chem. 2015, 26, 418−426

(11) Gillies, E. R., Jonsson, T. B., and Frechet, J. M. (2004) Stimuli-responsive supramolecular assemblies of linear-dendritic copolymers. *J. Am. Chem. Soc. 126*, 11936−11943.
(12) Mi, Y., Liu, Y., and Feng, S. S. (2011) Formulation of Docetaxel by folic acid-conjugated d-alpha-tocopheryl polyethylene glycol succinate 2000 (Vitamin E TPGS(2k)) micelles for targeted and synergistic chemotherapy. *Biomaterials 32*, 4058−4066.
(13) Xiao, K., Luo, J., Li, Y., Lee, J. S., Fung, G., and Lam, K. S. (2011) PEG-oligocholic acid telodendrimer micelles for the targeted delivery of doxorubicin to B-cell lymphoma. *J. Controlled Release 155*, 272−281.
(14) Matsumura, Y. (2014) The drug discovery by nanomedicine and its clinical experience. *Jpn. J. Clin. Oncol. 44*, 515−525.
(15) Ahn, H. K., Jung, M., Sym, S. J., Shin, D. B., Kang, S. M., Kyung, S. Y., Park, J. W., Jeong, S. H., and Cho, E. K. (2014) A phase II trial of Cremorphor EL-free paclitaxel (Genexol-PM) and gemcitabine in patients with advanced non-small cell lung cancer. *Cancer Chemother. Pharmacol. 74*, 277−282.
(16) Chang, Y., Kwon, Y. C., Lee, S. C., and Kim, C. (2000) Amphiphilic linear PEO−dendritic carbosilane block copolymers. *Macromolecules 33*, 4496−4500.
(17) Otsuki, T., Sakaguchi, H., Hatayama, T., Wu, P., Takata, A., and Hyodoh, F. (2003) Effects of all-trans retinoic acid (ATRA) on human myeloma cells. *Leuk Lymphoma 44*, 1651−1656.
(18) Xia, L., Wurmbach, E., Waxman, S., and Jing, Y. (2006) Upregulation of Bfl-1/A1 in leukemia cells undergoing differentiation by all-trans retinoic acid treatment attenuates chemotherapeutic agent-induced apoptosis. *Leukemia 20*, 1009−1016.
(19) Arce, F., Gatjens-Boniche, O., Vargas, E., Valverde, B., and Diaz, C. (2005) Apoptotic events induced by naturally occurring retinoids ATRA and 13-cis retinoic acid on human hepatoma cell lines Hep3B and HepG2. *Cancer Lett. 229*, 271−281.
(20) Wang, Q., Yang, W., Uytingco, M. S., Christakos, S., and Wieder, R. (2000) 1,25-Dihydroxyvitamin D3 and all-trans-retinoic acid sensitize breast cancer cells to chemotherapy-induced cell death. *Cancer Res. 60*, 2040−2048.
(21) Zhang, P., Huang, Y., Liu, H., Marquez, R. T., Lu, J., Zhao, W., Zhang, X., Gao, X., Li, J., Venkataramanan, R., Xu, L., and Li, S. (2014) A PEG-Fmoc conjugate as a nanocarrier for paclitaxel. *Biomaterials 35*, 7146−7156.
(22) Heard, C. M., Gallagher, S. J., Congiatu, C., Harwood, J., Thomas, C. P., McGuigan, C., Nemcova, M., and Nouskova, T. (2005) Preferential pi-pi complexation between tamoxifen and borage oil/gamma linolenic acid: transcutaneous delivery and NMR spectral modulation. *Int. J. Pharm. 302*, 47−55.
(23) Bottomley, A., Biganzoli, L., Cufer, T., Coleman, R. E., Coens, C., Efficace, F., Calvert, H. A., Gamucci, T., Twelves, C., Fargeot, P., and Piccart, M. (2004) Randomized, controlled trial investigating short-term health-related quality of life with doxorubicin and paclitaxel versus doxorubicin and cyclophosphamide as first-line chemotherapy in patients with metastatic breast cancer: European Organization for Research and Treatment of Cancer Breast Cancer Group, Investigational Drug Branch for Breast Cancer and the New Drug Development Group Study. *J. Clin. Oncol. 22*, 2576−2586.
(24) Zhang, Z., Mei, L., and Feng, S. S. (2013) Paclitaxel drug delivery systems. *Expert Opin. Drug Delivery 10*, 325−340.
(25) Gaucher, G., Marchessault, R. H., and Leroux, J. C. (2010) Polyester-based micelles and nanoparticles for the parenteral delivery of taxanes. *J. Controlled Release 143*, 2−12.
(26) Vader, P., Fens, M. H., Sachini, N., van Oirschot, B. A., Andringa, G., Egberts, A. C., Gaillard, C. A., Rasmussen, J. T., van Wijk, R., van Solinge, W. W., and Schiffelers, R. M. (2013) Taxol((R))-induced phosphatidylserine exposure and microvesicle formation in red blood cells is mediated by its vehicle Cremophor((R)) EL. *Nanomedicine (London) 8*, 1127−1135.
(27) Ihre, H., Padilla De Jesus, O. L., and Frechet, J. M. (2001) Fast and convenient divergent synthesis of aliphatic ester dendrimers by anhydride coupling. *J. Am. Chem. Soc. 123*, 5908−5917.
(28) Zhao, Y., Li, J., Yu, H., Wang, G., and Liu, W. (2012) Synthesis and characterization of a novel polydepsipeptide contained tri-block copolymer (mPEG-PLLA-PMMD) as self-assembly micelle delivery system for paclitaxel. *Int. J. Pharm. 430*, 282−291.
(29) Wu, Y., Chen, W., Meng, F., Wang, Z., Cheng, R., Deng, C., Liu, H., and Zhong, Z. (2012) Core-crosslinked pH-sensitive degradable micelles: A promising approach to resolve the extracellular stability versus intracellular drug release dilemma. *J. Controlled Release 164*, 338−345.
(30) Li, Y., Xiao, K., Luo, J., Xiao, W., Lee, J. S., Gonik, A. M., Kato, J., Dong, T. A., and Lam, K. S. (2011) Well-defined, reversible disulfide cross-linked micelles for on-demand paclitaxel delivery. *Biomaterials 32*, 6633−6645.
(31) Hong, G. Y., Jeong, Y. I., Lee, S. J., Lee, E., Oh, J. S., and Lee, H. C. (2011) Combination of paclitaxel- and retinoic acid-incorporated nanoparticles for the treatment of CT-26 colon carcinoma. *Arch. Pharm. Res. 34*, 407−417.
(32) Shahin, M., Ahmed, S., Kaur, K., and Lavasanifar, A. (2011) Decoration of polymeric micelles with cancer-specific peptide ligands for active targeting of paclitaxel. *Biomaterials 32*, 5123−5133.
(33) Kerns, E. H., Hill, S. E., Detlefsen, D. J., Volk, K. J., Long, B. H., Carboni, J., and Lee, M. S. (1998) Cellular uptake profile of paclitaxel using liquid chromatography tandem mass spectrometry. *Rapid Commun. Mass Spectrom. 12*, 620−624.
(34) Gillies, E. R., and Frechet, J. M. (2005) pH-Responsive copolymer assemblies for controlled release of doxorubicin. *Bioconjugate Chem. 16*, 361−368.
(35) Bae, Y., Fukushima, S., Harada, A., and Kataoka, K. (2003) Design of environment-sensitive supramolecular assemblies for intracellular drug delivery: polymeric micelles that are responsive to intracellular pH change. *Angew. Chem., Int. Ed. 42*, 4640−4643.
(36) Xiao, W., Luo, J., Jain, T., Riggs, J. W., Tseng, H. P., Henderson, P. T., Cherry, S. R., Rowland, D., and Lam, K. S. (2012) Biodistribution and pharmacokinetics of a telodendrimer micellar paclitaxel nanoformulation in a mouse xenograft model of ovarian cancer. *Int. J. Nanomedicine 7*, 1587−1597.
(37) Killoran, J., Allen, L., Gallagher, J. F., Gallagher, W. M., and O'Shea, D. F. (2002) Synthesis of BF2 chelates of tetraarylazadipyrromethenes and evidence for their photodynamic therapeutic behaviour. *Chem. Commun. (Cambridge)*, 1862−1863.
(38) Moore, J. S., and Stupp, S. I. (1990) Room temperature polyesterification. *Macromolecules 23*, 65−70.
(39) Zhan, C., Gu, B., Xie, C., Li, J., Liu, Y., and Lu, W. (2010) Cyclic RGD conjugated poly(ethylene glycol)-co-poly(lactic acid) micelle enhances paclitaxel anti-glioblastoma effect. *J. Controlled Release 143*, 136−142.
(40) Li, J., Guo, Y., Kuang, Y., An, S., Ma, H., and Jiang, C. (2013) Choline transporter-targeting and co-delivery system for glioma therapy. *Biomaterials 34*, 9142−9148.
(41) Murtagh, J., Frimannsson, D. O., and O'Shea, D. F. (2009) Azide conjugatable and pH responsive near-infrared fluorescent imaging probes. *Org. Lett. 11*, 5386−5389.
(42) Lu, H. L., Syu, W. J., Nishiyama, N., Kataoka, K., and Lai, P. S. (2011) Dendrimer phthalocyanine-encapsulated polymeric micelle-mediated photochemical internalization extends the efficacy of photodynamic therapy and overcomes drug-resistance in vivo. *J. Controlled Release 155*, 458−464.
(43) Hou, L., Yao, J., and Zhou, J. (2011) Simultaneous LC-MS analysis of paclitaxel and retinoic acidin plasma and tissues from tumor-bearing mice. *Chromatographia 73*, 471−480.

DOI: 10.1021/acs.bioconjchem.5b00030
Bioconjugate Chem. 2015, 26, 418−426